Chemical Physics Letters 495 (2010) 17–23

Contents lists available at ScienceDirect

Chemical Physics Letters

journal homepage: www.elsevier.com/locate/cplett

Photoionisation and structures of jet-formed toluene clusters

Tonia M. Di Palma [a,*], Attila Bende [b], Antonio Borghese [a]

[a] Istituto Motori – CNR, Via Marconi 8, 80125 Napoli, Italy
[b] Molecular and Biomolecular Physics Department, National Institute for R&D of Isotopic and Molecular Technologies, Donath Street, No. 65-103, RO-400293 Cluj-Napoca, Romania

ARTICLE INFO

Article history:
Received 23 April 2010
In final form 19 June 2010
Available online 23 June 2010

ABSTRACT

Here we report an experimental and computational study of toluene clusters that were formed in a He supersonic jet. A tunable vacuum ultraviolet radiation source was used to measure the ionisation potentials of dimers, trimers and tetramers from the onset of their photoionisation efficiency curves. DFT calculations were performed for different structures of stacked and non-stacked dimers and trimers as well as for a fully-stacked tetramer. Through comparison of the measured and calculated ionisation potentials, we show that under our experimental conditions, toluene nucleation starts from stacked dimers and proceeds through non-stacked trimers and tetramers.

1. Introduction

Molecular aggregates or clusters can be considered physical objects that bridge the transition from the gaseous to the condensed phase. They have been extensively studied in the last 30 years because the knowledge of their structure and energetics helps in the exploration of all macroscopic systems at the molecular level. Molecular clusters are the seeds of the nucleation process and are involved in key issues concerning aerosol formation in the Earth's atmosphere [1]. Moreover, cluster physics is the foundation of the increasingly important field of nanotechnology, with applications ranging from material science to biology [2].

Clusters of aromatic molecules are important systems for modelling molecular interactions in biomolecules and their solvation. The interaction between aromatic residues, usually termed π–π interactions, is often involved in specific, energetically favourable rearrangements such as base stacking in DNA or stabilisation in protein structures [3]. Most reports have been made on clusters of benzene [4], the archetypal aromatic molecule, because it is the simplest prototype for π–π interactions. Investigations of substituted benzene clusters are more complex due to the presence of substituents that introduce steric effects and dipole moments and often participate in hydrogen-bond interactions. Moreover, it has been shown that the methyl substituents on the benzene ring can act as hydrogen-bond donors [5] and, thus, provide a source of stabilisation in clusters containing aromatics.

The dynamics of toluene (TOL) clustering in a supersonic beam were first studied by Bernstein in the 1980s [6,7]. Recently, the toluene dimer $(TOL)_2$ has been proposed as the most realistic prototype for the π–π interaction in proteins. In particular, this model is well-suited for the study of the steric hindrances and dipole interactions in clusters [8]. Few studies have examined homogeneous toluene clusters. One experiment has been performed using vacuum ultraviolet (VUV) synchrotron radiation [9], wherein the ionisation potential (IP) and the dissociation energy were provided for the smallest toluene cluster, i.e., the toluene dimer. Recent RE-MPI experiments [10] have shown a close similarity between the absorption spectrum of the dimer and the absorption spectra of larger clusters; authors have found that there is little change in the bonding around the absorption site as the clusters grow. It has been proposed that the $(TOL)_2$ dimer unit is a stable entity, and that a dimer core is likely present in larger clusters. In addition, theoretical studies [11–13] have reported that stacked configurations that are parallel (PA), anti-parallel (PA) or crossed (CR) are the most stable dimer structures.

To assess the dynamics of cluster inception requires knowledge of the earliest structures that act as seeds for the later, larger ones. This Letter aims to compare experimental IP values of small $(TOL)_n$ clusters with those that were predicted by numerical modelling to shed light on the earliest seeding structures. To this end, we have used a tunable vacuum ultraviolet radiation from a laser produced plasma (LPP), we recently developed as soft single photon ionisation (SPI) source and coupled to time of flight mass spectrometry (TOF-MS) [14–16]. First, we experimentally determined the photoionisation efficiency (PIE) curves of toluene clusters $(TOL)_n$ that were spectrally resolved in the 8–10 eV range of ionising photon energy. We then inferred the ionisation potentials (IPs) of the first four toluene clusters ($n \leqslant 4$). Next, we performed DFT theoretical calculations for a set of structures corresponding to $(TOL)_n$ clusters with $n \leqslant 4$; the optimised geometric structures of toluene oligomers were obtained using the local version of second order Møller–Plesset perturbation theory (LMP2), whereas the IP values were calculated by considering the M06-2x DFT exchange-correlation functional. Finally, we compared these theoretical predictions to the experimental results and discussed our conclusions.

* Corresponding author. Fax: +39 0812396097.
E-mail address: t.dipalma@im.cnr.it (T.M. Di Palma).

0009-2614/$ - see front matter © 2010 Elsevier B.V. All rights reserved.
doi:10.1016/j.cplett.2010.06.053

2. Experimental

A detailed description of the experimental set-up has been reported in a previous paper [16]. However, for sake of completeness, a brief description is reported here. A sketch of the whole SPI–TOF-MS apparatus is shown in Fig. 1. The apparatus consists of two main vacuum chambers, each evacuated by its own turbomolecular pump (1000 l/s) and connected to a 1.04 m long flight tube. The VUV light source, based on laser produced plasma, was housed in the chamber on the right side of Fig. 1. A debris-free plasma was produced and by focusing a Nd-YAG laser (1064 nm, 10 ns and 200 mJ) onto a supersonic Xe gas jet emitted by a commercial solenoid valve (Parker mod. 99) with a back-pressure of 10 bar and an aperture time of 400 μs. The emitted radiation was first collected and then spectrally dispersed by a concave flat-field diffraction grating (70 mm diameter, 210 mm focal length and 8 nm/mm dispersion). Finally, the radiation was focused onto the sample molecular beam. In this configuration, vacuum ultraviolet (VUV) photon fluxes exceeding 10^{12}/cm^2 nm pulse (with 2% BW at 150 nm) were measured in the interaction volume [14].

In the same chamber, a second pulsed valve was used for the gas sample intake. A gaseous mixture of He and toluene vapour (Aldrich HPLC 99.9%+) at 2 bar and 25 °C was sent to the intake valve, which ejects a supersonic jet toward a 0.4-mm conical skimmer. A molecular beam was then selected coaxially to the TOF tube. The beam crossed the VUV optical axis at 90°. The skimmer was held directly on the wall of an inner chamber (i.d. of 60 mm) containing MgF_2 windows. This inner chamber housed the extraction fields (see Fig. 1) in such a way as to shorten the distance between the valve nozzle and the ionisation region to 70 mm.

The mass spectrometer was a homemade linear TOF spectrometer. The spectrometer consisted of a Wiley Mc-Laren instrument equipped with ion optics (x–y deflection plates, an Einzel lens and a 2-mm pin hole), which allowed us to control the ion collection at the channeltron detector (Burle mod. 4821G). The mass resolution was $m/\Delta m \approx 200$ at $m/z = 92$ by using a constant extraction field of 200 V/cm and could be increased at $m/\Delta m \approx 420$ at $m/z = 128$ (naphthalene) by using pulsed/delayed extraction fields [16].

In this configuration, the spectral resolution achievable for the photon wavelength was a function of the grating dispersion (8 nm/mm) and of the transverse sizes of the LPP [14] and the molecular beam. The overall value of the resolution was determined by recording the mass spectra intensities while scanning the zeroth order reflection of the grating, i.e., the LPP shape across the molecular beam. We measured a line width of approximately 0.8 mm (FWHM), corresponding to a wavelength resolution of approximately ±3 nm (±0.2 eV at 9 eV) for the first order of the grating and approximately ±1.5 nm (±0.1 eV at 9 eV) for the second order of the grating.

A stepping motor was used for spectral scanning and a LabVIEW-driven DAQ card (National Instruments, PCI-5152) was used for data acquisition. Typically, 500 shots were accumulated to give one mass spectrum at each wavelength. Mass spectra shown here were sequentially acquired using 0.4-nm steps over the second order of the spectral band at 124–155 nm (10.0–8.0 eV). The photoionisation efficiency (PIE) spectrum of each cluster was obtained by plotting the area of the corresponding mass peak as a function of its ionising photon energy. The photoionising energy scale was calibrated using the appearance energy of the ion $C_4H_{10}O^+$ at 9.6 eV corresponding to the contaminant diethyl ether at $m/z = 74$ and its fragment, $C_3H_7O^+$ ($m/z = 59$), at 10.6 eV [17]. Data presented here were not corrected for the VUV intensity, as its variation was less than 10% in the explored spectral range of 8.0–10.0 eV.

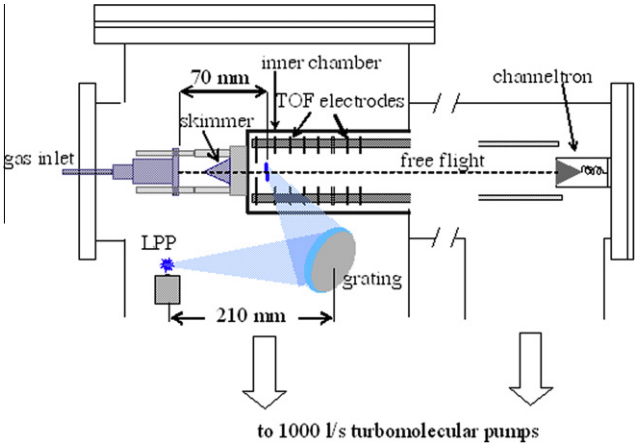

Fig. 1. Experimental layout of the tunable SPI–TOF apparatus (see text). The TOF mass spectrometer was equipped with extraction/acceleration electrodes and seven cascaded focusing electrodes. The electric-field settings were: $E_{ext} = E_{acc} = 200$ V/cm and $E_{foc} = 257$ V/cm. The TOF free-field length was 96 cm. The details of the laser plasma-grating geometry are reported in Refs. [14,15].

3. Theoretical methods

The equilibrium geometry of the dimer, trimer and tetramer structures of toluene, the intermolecular interaction energies of dimer structures and the relative configuration energies for the trimer structures were obtained by considering the local version of second order Møller–Plesset perturbation theory (LMP2) combined with the density fitting (DF) technique [18–20]. These calculations were implemented using the Molpro program package suite [21] and the *aug-cc-pVTZ* basis set. Using the program parameter descriptions as presented in past research [22,23], we employed the following input settings: (i) instead of using the Pipek–Mezey localisation procedure [24], we considered the natural localised molecular orbitals (NLMO) [23] because NLMOs are much less sensitive to the basis set, in particular when diffuse functions are used; (ii) to overcome poor orbital localisation in the NLMO technique when larger diffuse basis sets were used, we eliminated the contribution of the diffuse basis functions to the localisation criteria by setting the corresponding rows and columns of the overlap matrix used in the NLMO localisation to zero; and (iii) the domains of the three aromatic π-orbitals in each benzene-type ring were merged, leading to three identical domains that included the p_π atomic orbitals of all six carbon atoms from the given six-membered ring. With regard to the fact that the DF-LMP2 method is only applicable to closed-shell systems, the ionisation potential values were calculated using the M06-2x [25] DFT exchange-correlation functional as implemented in the Nwchem program suite [26] using the *aug-cc-pVDZ* basis set. Based on the results obtained with high correlation methods and large basis sets, the parameterisation of the M06-2x XC functional was extended within the van der Waals region. A test benchmark was presented by Korth and Grimme [27]. They found that the mean absolute deviation obtained with different DFT functionals decreased very strongly because of the local density approximation (LDA) used for GGAs, but that this decrease was less pronounced with meta-hybrid-GGAs such as M06-2x. This phenomenon is particularly relevant for π-stacking molecular systems.

4. Results

4.1. Experimental results

The extent of cluster formation in a supersonic expansion depends on the local gas temperature and its concentration and is

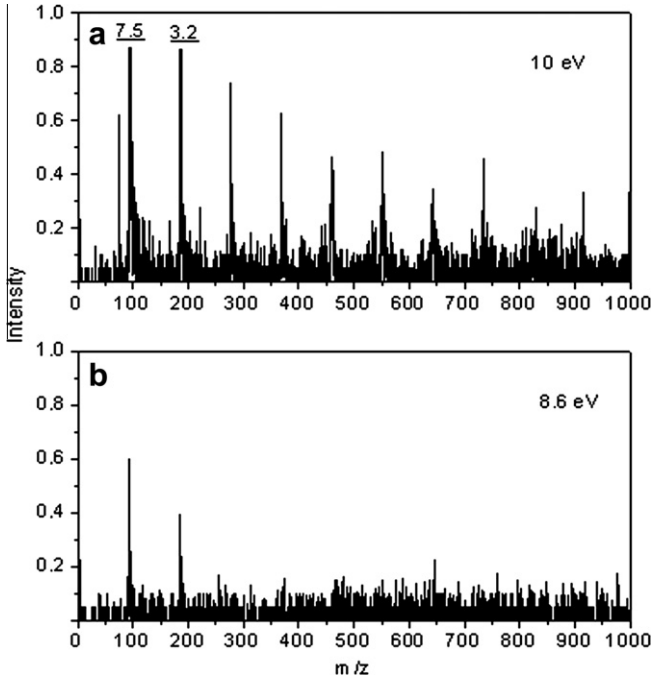

Fig. 2. Mass spectra of toluene clusters detected at (a) 10.5 eV (upper spectrum) and (b) 8.6 eV (bottom spectrum).

easily tuned by choosing appropriate time delays between the jet onset and the ionising photon pulse. With short delays, the leading edge of the molecular beam in which the gas concentration is low is probed, and only monomers and dimers are detected with peak intensity ratios of nearly 10:1. A wider cluster distribution appears at longer delays. We have chosen to use a 50-μs delay in the ionising light pulse so that we can detect the onset of the clusters' distributions. The mass spectra reported in Fig. 2a and b refer both to this latter gas-dynamic conditions and acquired at two particular values of the photoionising energy: 10.0 eV, well above the appearance energy of the $(TOL)_n$ clusters (Fig. 2a), and 8.6 eV, just above the appearance energy of the $(TOL)_2$ dimer (Fig. 2b). In the former spectrum, clusters with up to 10 toluene molecules were ionised by the 10.0-eV photons. In the latter spectrum, only monomers and dimers were ionised by the 8.6-eV photons.

Fig. 3a–d shows the PIE spectra of the clusters $(TOL)_n$ with $n = 1–4$ that were retrieved from the mass spectra collected in the gas-dynamic conditions of Fig. 2a and b by scanning the second order of the radiation across the range of 8.2–10.0 eV. The monomer's PIE spectrum in Fig. 3a shows a flat background below 8.6 eV and increases with constant slope above this value. The background signal is likely due to molecules ionised by VUV stray-light and/or secondary electrons. The PIE curve's onset of the toluene monomer falls at 8.8 ± 0.1 eV, which is in agreement with the toluene IP recorded in the NIST database [17]. Fig. 3b shows the PIE curve of the toluene dimer $(TOL)_2$ that has an onset at approximately 8.5 ± 0.1 eV. Fig. 3c and d shows the PIE curves of the trimer $(TOL)_3$ and the tetramer $(TOL)_4$, which have onsets at nearly the same values as the dimers within our experimental accuracy. It is worth noting that the experimental data for larger clusters are affected by larger error due to their lower signal-to-noise ratios. However, we reproduced the same results in the PIE spectra acquired through the use of first order VUV radiation (data not shown) in which we observed half of the value of energy resolution and a fourfold increase in the signal-to-noise ratio.

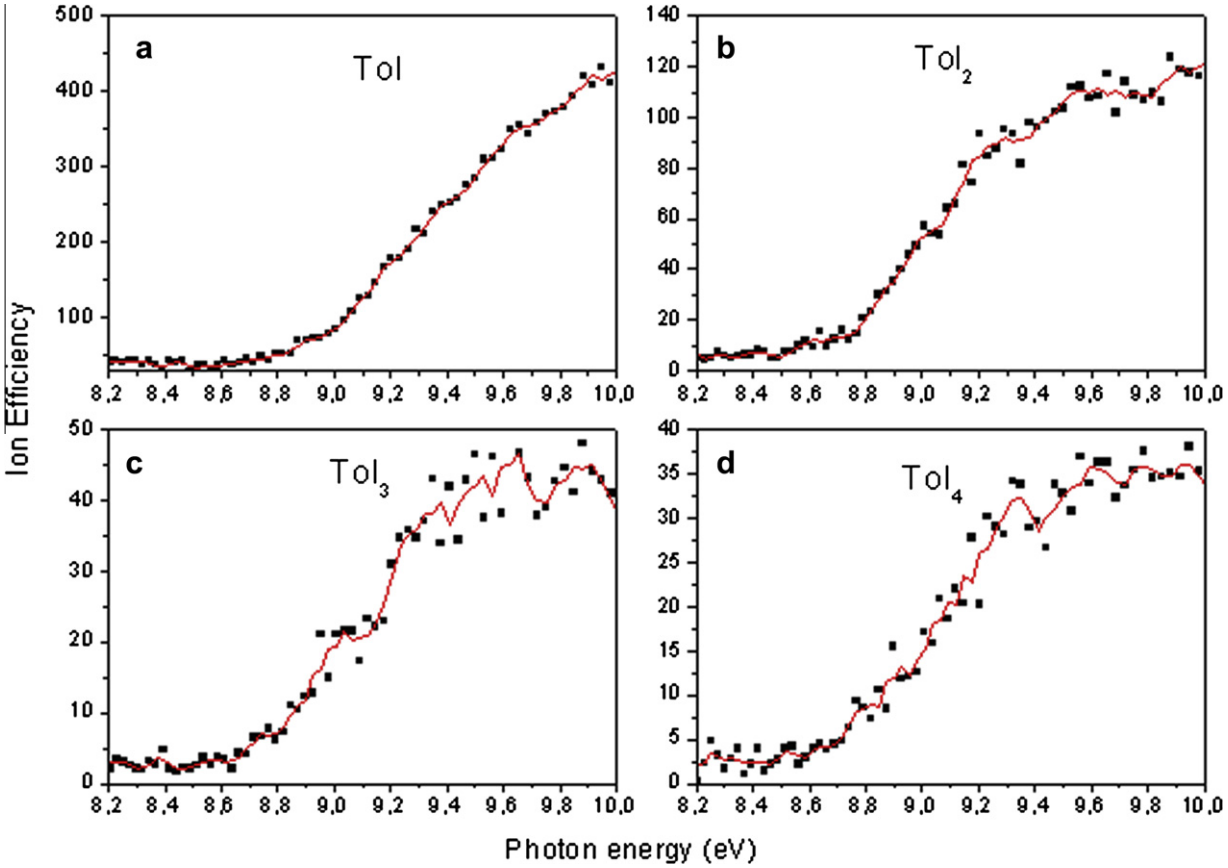

Fig. 3. Photoion yield efficiency spectra of TOL_n with $n = 1, 2, 3$ and 4.

4.2. DFT calculations

The shape of the PIE curves near threshold depends mainly on the possible isomer distribution, the cluster temperature and Frank-Condon factors [28]. In particular, the last two effects give rise to low-energy tails in the PIE spectra which require a thorough analysis of the measurements to determine adiabatic and vertical ionisation potentials. Usually, the IPs measured in photoionisation experiments fall below the vertical IPs and approach the adiabatic ones as the sensitivity increases [29]. Due to our experimental sensitivity, the onset in our PIE spectra is interpreted as closer to the vertical IP [30]. Such value is obtained by using computational methods based on the energy difference between the neutral cluster and the ionised cluster, keeping the neutral cluster's ground-state molecular geometry. The comparison of the calculated vertical IP with the experimental IP allows us to determine what the most likely cluster structure is.

Despite many studies that have used *ab initio* calculations to examine toluene dimers [11–13], no work has examined larger clusters due to the vast number of structures that must be considered in such calculations. The results of *ab initio* calculations suggest that for the toluene dimers, stacked structures are preferred over T-shaped structures. Recent spectroscopic work [10] suggests that dimers are formed preferably in the stacked structure, and that larger clusters may be built around a stable dimer as the core. We performed *ab initio* calculations on the toluene oligomers $(TOL)_n$ with $n = 2–4$ by assuming a stacked configuration for all cases. In addition, for the dimer and trimer only, the analysis was extended to non-stacked geometries.

4.2.1. The toluene dimer structures

The geometry optimisation using the theoretical level of DF-LMP2 theory level and the *aug-cc-pVTZ* basis set led to three equilibrium configurations of the toluene dimers. This result is similar to the findings presented by Tsuzuki et al. [12] and Rogers et al. [13]. The most stable dimer was found in the anti-parallel (AP) configuration (Fig. 4a), followed by the parallel (PA) stacking configuration (Fig. 4b). The cross (CR) dimer structure had the weakest bound form (Fig. 4c). Alternative starting geometries were also constructed to investigate the T-shape configuration of the toluene dimer. The geometry optimisation proved to us that no stable T-shape dimer structure existed in the stacking parallel form. This fact confirmed the studies of Gervasio et al. [11] and Rogers et al. [13]. Because open shell calculations are not available to us while we are using the DF-LMP2 level of theory, the ionisation potential values were calculated using the M06-2x highly parametrised hybrid meta-GGA XC functional with the DFT level of theory. Through consideration of different benchmark studies using molecular databases, Zhao and Truhlar [25] have demonstrated that the M06-2x XC functional performs well in describing π-stacking systems, including for intermolecular interactions, ionisation potentials, and electron and proton affinities. According to their work, the experimental IP values in the case of π-stacking systems are usually found to be theoretically reproduced with only a minor difference of 0.1–0.2 eV. The intermolecular interaction energies, the vertical ionisation potentials and the geometry parameters calculated with different theoretical methods are presented in Table 1. For the IP calculation, the M06-2x/aug-cc-pVDZ calculation level was applied by using the geometry structure obtained with the DF-LMP2/aug-cc-pVTZ method. By comparing the intermolecular interaction energies obtained at different levels of theory, one can see that the dimer structures are exclusively stabilised by electron correlation effects because the HF contribution has only very small repulsive effects. This repulsion is outweighed by a stronger attractive action of the electron correlation, and, thereby, a bound dimer is formed. The electron correlation contribution is approximately 13.2 kcal/mol for PA and CR configurations, which is larger by approximately 2.0 kcal/mol than the AP case. However, the HF contributions are also higher, which finally leads to a slightly weaker bound structure. For the AP and PA cases, it was observed that when compared with the DF-LMP2 and DF-LCCSD(T) methods, the M06-2x slightly underestimated the interaction energy values, whereas in the CR case, this discrepancy was large. By considering the ionisation potential results for different stacking configurations, we found only small deviations in their values; all three vertical IPs were close to 8.5 eV.

Table 1
The intermolecular interaction energy obtained at the HF, DF-LMP2, DF-LCCSD(T) and M06-2x theoretical levels using the *aug-cc-pVDZ* basis set. Additionally, the ionisation potentials and the stacking plane distances for anti-parallel, parallel and cross stacking toluene dimers are shown.

	AP stacking	PA stacking	CR stacking
ΔE^{HF} (kcal/mol)	2.505	5.174	5.093
ΔE^{LMP2} (kcal/mol)	−8.640	−8.000	−8.202
$\Delta E^{LCCSD(T)}$ (kcal/mol)	−8.308	−7.970	−7.884
$\Delta E^{M06\text{-}2x}$ (kcal/mol)	−7.476	−6.732	−5.885
$IP^{M06\text{-}2x}$ (eV)	8.480	8.513	8.510
Plane distances (Å)	3.407	3.404	3.333

4.2.2. The toluene multi-stacking systems

To study the IP trends for the most stable dimer system (the anti-parallel configuration), we have examined the higher oligomer stacking of toluene trimers and tetramers, as shown in Fig. 5. The geometry structures were optimised using the DF-LMP2 level of theory and the *aug-cc-pVTZ* basis set. For the trimer system, we found perfect parallel stacking planes of the six-membered rings, whereas for the tetramer system, the third and the fourth planes were tilted by approximately 8° from the plan-parallel configuration. This effect could be explained through involvement of long-range attractive forces between distant monomers. The vertical IP values were again obtained using the M06-2x DFT functional and the *aug-cc-pVDZ* basis set. These values were 8.224 eV for the trimer configuration and 8.104 for the tetramer

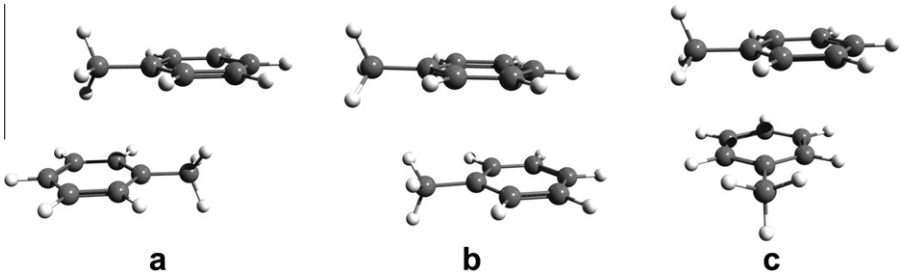

Fig. 4. The anti-parallel (a), parallel (b) and cross (c) structures of the stacking toluene dimers.

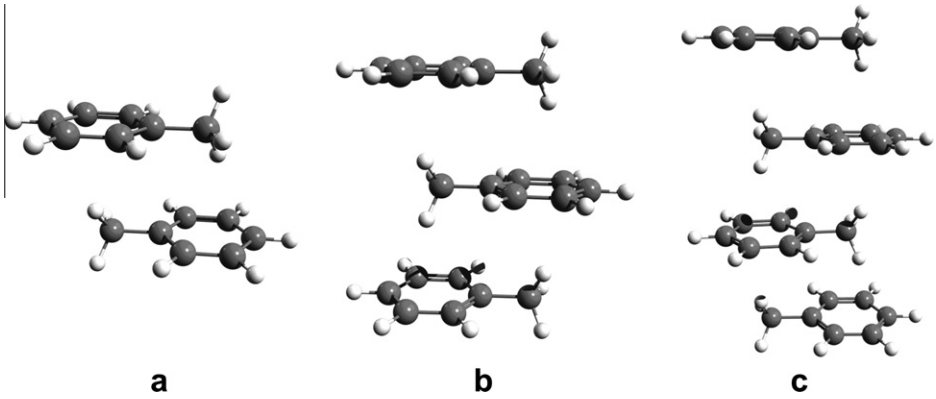

Fig. 5. The dimer (a), trimer (b) and tetramer (c) stacking configurations of the toluene cluster.

case, which displayed a decreasing tendency of IP values as the number of stacking planes increased. Through analysis of the HOMO orbitals in the case of neutral stacking and the alpha and beta spin-orbitals for the ionised stacking systems, one can conclude that for the trimer and tetramer configurations, the ionised electrons originated from the middle monomers, whereas in case of the dimers, the ionisation affected both monomer orbitals in a same manner.

4.2.3. The trimer toluene stacking systems

To investigate the cluster properties of the toluene oligomers, we performed a comprehensive analysis of toluene trimers. Based on the toluene dimer geometry configurations, we built three different trimer configurations in which the extant anti-parallel, parallel and cross dimer configurations involving the third monomer were placed randomly. These configurations are referred to as Trim I, Trim III and Trim IV, and their geometry-optimised structures were obtained with the DF-LMP2 level of theory using the *aug-cc-pVTZ* basis set as shown in Fig. 6. Two more trimer structures were designed (Trim II and Trim V) in which we tried to investigate the stability of the triangular form of the toluene monomers. The geometry optimisation of these two structures showed us that they were also stable trimer configurations. The vertical IPs were obtained in the same manner as in the previous two sections, namely, by considering the M06-2x/aug-cc-pVDZ calculation level. Accordingly, the five structures were labelled according to their ascendant energy differences between their total energy and the reference energy of the trimer stacking ($\Delta E = E^{\text{stack}} - E^{\text{i}}$). The configuration energies and vertical IPs of these trimers are collected in Table 2.

By analysing the configuration energy of the above-mentioned five trimer configurations by comparing them with the tri-stacking toluene value, one can observe that these differences are usually between 1.8 and 2.5 kcal/mol except for the Trim V configuration for which we found 5.1-kcal/mol energy differences. Further, the vertical IPs were between 8.27 and 8.41 eV for the first four

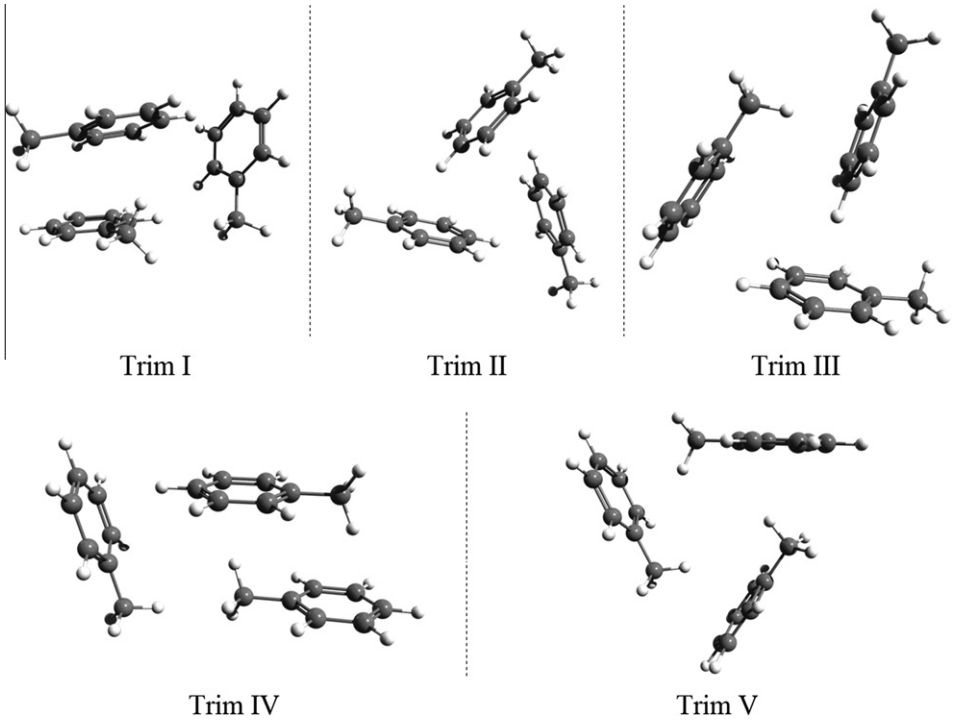

Fig. 6. Five different configurations of the toluene trimer.

Table 2
The configuration energies and the vertical IPs for different toluene trimers.

Configuration	ΔE (kcal/mol)	IP* (eV)
Trim I	−1.811	8.332
Trim II	−2.050	8.267
Trim III	−2.106	8.406
Trim IV	−2.536	8.395
Trim V	−5.070	8.484

* The IP of the stacking toluene trimer is 8.224 eV.

complexes and 8.48 eV for the Trim V system. Based on these findings, one can conclude that the tri-stacking system has the lowest IP value, whereas other trimer configurations have higher IPs between 0.1 and 0.2 eV with respect to the tri-stacking system.

4.3. Discussion

The formation of dimers with stacked geometries has been confirmed in this Letter, as the experimental IP of 8.5 ± 0.1 eV is similar to the predicted values of 8.48 eV for stacked AP and 8.51 for stacked PA and CR geometries.

For higher-order clusters, Musgrave and Wright [10] observed a similarity in the REMPI spectra for dimer and larger clusters and advanced the hypothesis that a stable dimer unit is always present in clusters with $n > 2$. Correspondingly, we measured the same energy values at the ionisation threshold for toluene clusters with $n \geqslant 2$, which led to support for the hypothesis that stacked dimeric units exist in the larger clusters. In addition, our DFT calculations for a variety of geometries of trimers and a fully-stacked tetramer suggest that this hypothesis is correct. In fact, from the comparison of the measured IPs with the calculated ones for the trimer and tetramer, we deduced that low-energy trimers and tetramers with ordered, fully-stacked structures are not formed under expansion condition because, in both cases, the measured IPs (8.6 ± 0.1 eV) were far higher that the calculated ones (8.2 ± 0.2 eV and 8.1 ± 0.2 eV, respectively). Instead, the high-energy, partially-stacked configurations of the trimers termed Trim I, Trim III and Trim IV, which include a stacked dimer structure bound to a non-stacked monomer, yielded IPs of 8.33, 8.41 and 8.39 eV, respectively. Taking into account the ±0.2 eV expected error, these IP values are in agreement with the experimental data. On the other hand, the Trim V configuration that is described by a triangle-shaped, head-to-tail linked arrangement (see Fig. 6) has an IP of 8.48 eV, which is closer to the experimental value than the other shapes even though it is less stable than the others.

It is worth noting that the formation of high-energy isomers is a well-known occurrence in supersonic jet expansion, and, frequently, experimentally-identified isomers are different from those of lower-energy as predicted by *ab initio* calculations [31]. This phenomenon suggests that there is a low incidence of the collisional relaxation during the free jet expansion phase, as demonstrated by Ruoff et al. [32] in experiments on different conformers and isomers seeded in a supersonic jet. They found that conformers with barriers to internal rotation that were greater than or equal to 400 cm^{-1} (about 1 kcal/mol) did not relax significantly in any gas carrier used for the expansion. Instead, they found that the conformers were 'frozen' in high-energy structures that formed during an early stage of the expansion. Similar conclusions were found for the relaxation of weakly-bound clusters. In our case, the toluene was seeded in helium, which is less effective than other noble gases in causing relaxation [32]. In addition, we found the relative configuration energies to be between 1.8 and 5.1 kcal/mol for the non-stacked trimers. Therefore, it is reliable that, when a single molecule sticks on a stacked dimer in a random direction, the formed trimer is frozen with a structure that resembles the structures presented herein. Similar reasoning led us to suppose that the tetramers that were formed from the sticking of molecules onto non-stacked trimers in random direction were frozen in the beam with non-stacked structures. Hence, we are led to believe that the nucleation of toluene oligomers can only occur through the sticking of non-stacked monomers on stacked dimers, which is followed by successive growth of the random structures.

5. Conclusion

A picture of the inception of toluene clustering has been described by combining mass spectrometry, photoionisation efficiency data and DFT calculations. New data regarding the photoionisation ion yield of toluene clusters of sizes up to tetramers have been presented. We have found that IP values of oligomers with up to four toluene molecules are not lower than about 8.5 eV. We have performed *ab initio* calculations for stacked dimers, trimers built from stacked and non-stacked structures and a stacked tetramer and have compared the experimental values of their PIE curve onsets with IPs calculated for the modelled clusters. We have found that the onset of the dimers' PIE spectra agree with the IPs predicted for the stacked dimers. The IP values predicted by DFT for trimers and the tetramer with fully-stacked geometries are much lower than those observed experimentally. A fair agreement has been found for non-stacked trimers, which include at most one stacked dimer. We conclude that under our experimental conditions, toluene aggregation starts from stacked dimers and proceeds through non-stacked geometries.

Acknowledgements

The authors wish to thank the technical support of Mr. B. Sgammato. T.M. Di Palma acknowledges financial support from 'Ricerca Spontanea a Tema Libero' (*Curiosity Driven Research*) Grant No. 326 of the Italian National Research Council. The theoretical calculations were performed in the Data Centre of NIRDIMT Cluj-Napoca for which we express our grateful acknowledgment.

References

[1] M. Kulmala, Science 302 (2003) 1000.
[2] A.W. Castleman Jr., Puru Jena, Proc. Natl. Acad. Sci. 103 (28) (2006) 10554.
[3] S.K. Burley, G.A. Petsko, Science 229 (1985) 23.
[4] C.Y. Ng, Vacuum Ultraviolet Photoionization and Photodissociation of Atoms and Clusters, World Scientific Publisching Co. Pte. Ltd., 1991.
[5] P. Hobza, V. Spirko, H.L. Selze, E.W. Schlag, J. Phys. Chem. A102 (1998) 15.
[6] D.W. Squire, R.B. Bernstein, J. Phys. Chem. 88 (21) (1984) 4944.
[7] K.S. Law, M. Schauer, R.B. Bernstein, J. Chem. Phys. 81 (11) (1984) 4871.
[8] C. Chipot, R. Jaffe, B. Maigret, D.A. Pealman, P.A. Kollman, J. Am. Chem. Soc. 118 (1996) 11217.
[9] E. Rühl, P.G.F. Bisling, B. Brutschy, H. Baumgärtel, Chem. Phys. Lett. 126 (3–4) (1986) 232.
[10] A. Musgrave, T.G. Wright, J. Chem. Phys. 122 (2005) 074312.
[11] F.L. Gervasio, R. Chelli, P. Procacci, V. Schettino, J. Phys. Chem. A 106 (12) (2002) 2945.
[12] S. Tsuzuki, K. Honda, T. Uchimaru, M. Mikami, J. Chem. Phys. 122 (2005) 144323.
[13] D.M. Rogers, J.D. Hirst, E.P.F. Lee, T.G. Wright, Chem. Phys. Lett. 427 (2006) 410.
[14] A. Borghese, T.M. Di Palma, Appl. Opt. 46 (22) (2007) 4951.
[15] T.M. Di Palma, A. Borghese, Nucl. Instrum. Methods Phys. Res. B 254 (2007) 193.
[16] T.M. Di Palma, M.V. Prati, A. Borghese, J. Am. Soc. Mass Spectrom. 20 (12) (2009) 2192.
[17] http://webbook.nist.gov/chemistry/.
[18] P. Pulay, Chem. Phys. Lett. 100 (1983) 151.
[19] C. Hampel, H.-J. Werner, J. Chem. Phys. 104 (1996) 6286.
[20] M. Schütz, H.-J. Werner, J. Chem. Phys. 114 (2001) 661.
[21] H.-J. Werner, et al., Molpro, Version 2008.1, A Package of *ab initio* Programs, Available from: <http://www.molpro.net>.
[22] J.G. Hill, J.A. Platts, H.-J. Werner, Phys. Chem. Chem. Phys. 8 (2006) 4072.
[23] R.A. Mata, H.-J. Werner, Mol. Phys. 105 (19–22) (2007) 2761.
[24] J. Pipek, P.G. Mezey, J. Chem. Phys. 90 (1989) 4916.

[25] Y. Zhao, D.G. Truhlar, Theor. Chem. Acc. 120 (2008) 215.
[26] E.J. Bylaska, et al., NWCHEM, A Computational Chemistry Package for Parallel Computers, Version 5.1.1, Pacific Northwest National Laboratory, Richland, Washington, USA, 2009.
[27] M. Korth, S. Grimme, J. Chem. Theory Comput. 5 (2009) 993.
[28] G.N. Makarov, Phys. Usp. 51 (4) (2008) 319.
[29] H.L. Selzle, H.J. Neusser, B. Ernstberger, H. Krause, E.W. Schlag, J. Phys. Chem. 93 (1989) 7535.
[30] H. Baungartel, B. Brutschy, E. Ruhl, Phys. Scr. T31 (1990) 78.
[31] P.D. Godfrey, R.D. Brown, F.M. Rodgers, J. Mol. Struct. 376 (1996) 65.
[32] R.S. Ruoff, T.D. Klots, T. Emilsson, H.S. Gutowsky, J. Chem. Phys. 93 (5) (1990) 3142.